First principles site occupation and migration of hydrogen, helium, and oxygen in β-phase erbium hydride

R.R. Wixom[1,*], J.F. Browning[2], C.S. Snow[1], P.A. Schultz[1], and D.R. Jennison[1].

[1]*Sandia National Laboratories, Albuquerque, NM 87185*

[2]*Oak Ridge National Laboratory, Oak Ridge, TN 37831*

ABSTRACT

First principles density functional methods were used to investigate the atomistic behavior of hydrogen, helium, and oxygen in β-phase ErH_2. The ground-state for hydrogen was indeed determined to be the tetrahedral position as commonly assumed, but if the surrounding tetrahedral sites are filled any additional hydrogen will occupy the octahedral site. Only a small amount of thermally generated tetrahedral-vacancy octahedral-occupancy pairs are predicted at equilibrium since the barrier and formation energies are 1.90 and 1.21 eV respectively. Two other possible scenarios will result in octahedral hydrogen occupation, a H/Er ratio > 2.0 and the presence of oxygen in the lattice. Our calculations indicate that oxygen impurities will reside in tetrahedral sites, even if that site is already occupied and hydrogen must be displaced into a neighboring octahedral site. Oxygen will migrate at moderate temperatures by jumping between tetrahedral sites and octahedral sites. The extent of hydrogen self-diffusion will depend on the concentration of tetrahedral vacancies and/or octahedral hydrogen and therefore will be enhanced by overloading hydrogen or the presence of significant oxygen contamination. In samples where some of the hydrogen is replaced with tritium, helium generated by tritium decay will favor a tetrahedral site left vacant by a transmuted tritium. The barrier to migration between two unoccupied neighboring tetrahedral sites is

0.49 eV, where the path maximum corresponds to the octahedral site. If an extended network of neighboring vacancies exists, the relatively small barrier provides that helium may move throughout that at room temperature. Given enough energy to escape the tetrahedral site(s), 1.31 eV, helium may continue to migrate by a 0.88 eV concerted-motion mechanism---temporarily displacing hydrogen as it moves between empty octahedral sites and filled tetrahedral sites.

I. INTRODUCTION

Rare earth metal hydrides readily absorb hydrogen, and for this reason they are obvious candidate materials for certain applications that require long term stable storage of hydrogen isotopes. One such application is the neutron tube, which utilizes either deuterium-deuterium (D+D) or deuterium-tritium (D+T) reactions to produce neutrons. Erbium hydride (or other metal-hydrides) can be used to hold the tritium and deuterium until they are needed for the neutron generating reaction. For tritium containing designs, the relatively short half-life of tritium (12.3 years) introduces very interesting materials science challenges due to the resulting production of helium via the reaction $T \rightarrow {}^{3}He + \beta^{-} + \bar{\nu}$, where β^{-} is a beta particle and $\bar{\nu}$ is an anti-neutrino. For vacuum devices, like the electrostatic accelerator neutron tube, helium evolving from the tritium-containing material degrades the vacuum, which can be catastrophic to functionality. Compact neutron sources have a variety of uses including the identification of concealed explosives and several geological applications such as detection of subsurface water, oil, and minerals.

Early in the life of erbium tritide, small amounts of helium will escape from the near surface regions.[1] Later, when the helium concentration becomes large enough, plate-like helium bubbles form, which are observable in transmission electron micrographs (TEM).[1] Eventually, the concentration of helium reaches the point of 'critical release,' where wholesale escape of helium occurs. Beyond these empirical observations, our understanding of the behavior of helium in this material is in its infancy. As such,

intriguing questions remain regarding the atomistic nature of the material itself, helium bubble nucleation and growth, and the consequences of impurities. Experimental studies of the transient material properties resulting from tritium decay are extremely time consuming, expensive, and difficult. The allure of theoretical investigations is to mitigate these difficulties while gaining quantitative insight into the fundamental physical processes that drive the macroscopic behavior. In this study, we investigate migration of hydrogen, helium and oxygen in erbium tritide, using first principles calculations within density functional theory (DFT).

II. COMPUTATIONAL DETAILS

The exchange-correlation functional we used for this DFT study was the generalized gradient approximation (GGA) of Perdew, Burke, and Ernzerhof (PBE).[2] The calculations were performed with SeqQuest,[3] using standard (semi-local) norm-conserving pseudopotentials, and well-optimized double-zeta plus polarization contracted Gaussian basis sets. The oxygen atom pseudopotential was generated using the Troullier-Martins method,[4] the helium and erbium atoms used the generalized norm-conserving pseudopotentials of Hamann,[5] all using the fhi98PP code.[6] The H pseudopotential was generated using a new method by Hamann.[7] Additional calculations, as noted in the text, were performed with the Vienna *ab initio* Simulation Package (VASP).[8] These involved the projector augmented wave (PAW) method, where the PAW potentials were taken from the VASP database,[9] and used a plane wave basis with a kinetic energy cutoff of 400 eV (700 eV for calculations containing oxygen).

Lanthanides can be problematic for DFT calculations and are not frequently the subject of pseudopotential studies. Hence, it is necessary to discuss the details of how the erbium pseudopotentials, used in the SeqQuest calculations, are constructed and verified. First, we note that the magnetic properties of Er are not pertinent to the chemistry we examine, and further note that the oxidation state of erbium (the number of *f*-electrons) will not change. The *f*-electrons, being very near the core, are expected to be chemically inert. We take advantage of this observation to remove the *f*-electrons on the erbium atom, along with the computational difficulties associated with them, from the valence, and construct our erbium pseudopotential treating 11 *f*-electrons as core electrons. It proved necessary to keep the six semi-core 5*p* electrons as valence electrons; we were unable to converge construction of a $5p^6$-core pseudopotential to reproduce results from $5p^6$-valence pseudopotentials. The non-linear exchange-correlation effects on the valence electrons due to the remaining core electrons was included via a partial core correction [10], converged at a matching radius of 2.0 bohr. We used an atomic +0.5 cation, $[(Xe\text{-}5p^6)f11]5p^6 5d^{2.0} 6s^{0.5}$, for constructing the erbium pseudopotential. Default radial parameters were used to construct each angular momentum channel.

These new pseudopotentials were first tested on bulk erbium. Erbium is an hcp metal, with lattice constants a=3.56 Å and c=5.59 Å. Using the local density approximation (LDA), the fcc structure was equally stable as hcp, within ~1 meV/Er (using a 16^3 k-sample for the fcc, and a 16x16x10 k-sample for the hcp crystal), indicating that LDA might have difficulties modeling chemistry involving erbium. Furthermore, the

optimized hcp lattice parameters with LDA, a=3.440 Å and c=5.374 Å, were in rather poor agreement with experiment. The LDA c/a ratio of 1.565 was good, but the lattice is 3.5% too small. As we are interested in barrier energies, and the helium barriers are mostly steric, the too-small erbium atoms in LDA could likely lead to significantly overestimated barrier heights for helium migration. This is what motivated the use of the PBE approximation in this study. The PBE lattice parameters for the Er hcp structure were computed to be a=3.549 Å and c=5.562 Å, with c/a=1.567, all in very good agreement with experiment. Just as important, the hcp structure is clearly the ground state, the fcc structure being 25 meV/Er higher in energy than hcp with PBE.

The computational defect models were based on 96-site cubic supercells, a 2x2x2 scaling of the 12-atom cubic representation of the ground state β-ErH_2 crystal, to which atoms were removed, added, or replaced to generate models of the desired defects. A {4,4,4} (n_{MP}=4) Monkhorst-Pack [11] grid was used to sample the Brillouin Zone. Convergence of these supercell models with respect to larger n_{MP}, and higher plane wave energy cutoff was confirmed in VASP calculations.

The computed equilibrium lattice parameters for β-ErH_2 were 5.115 Å with SeqQuest and 5.129 Å with VASP, both in good agreement with each other and with the experimental value 5.126 Å.[12] The agreement between SeqQuest and VASP results continues throughout the numerical results presented in this paper. In the calculations repeated by both codes, a typical difference in the results was 0.02 eV. Given that these are very different codes, using different basis sets and atomic potentials, this lends

confidence to the construction of the computational models for Er, and, in particular, verifies the construction of the pseudopotentials.

Local energy minimum atomic configurations were obtained from a chosen starting configuration by moving each atom along the direction of the force on that atom, iterating until the magnitude of the force on every atom was less than 0.01 eV/Å. The ground state and meta-stable states were assigned by comparing the total energies corresponding to different local minima. The climbing image nudged elastic band method (CI-NEB) [13] was used to determine transition state configurations and to compute barrier energies for diffusion. The CI-NEB constructs a series of atomic configurations along a minimum energy path transitioning between the atomic configurations corresponding to neighboring local minima. The transition state corresponds to the highest energy point along this path, to which the climbing image—the transition state configuration—has ascended. The migration barrier energy is the difference between this transition state total energy and the total energy of the nearby local minima.

The barrier energies (E_a) obtained by CINEB were used to make qualitative estimates of diffusion lengths L, where $L = (6Dt)^{1/2}$, and $D = D_o \exp(-E_a/kT)$. In these equations, t is the time, T is temperature, k is the Boltzmann constant, and D_o is a frequency factor. In the absence of first principles values for D_o, we have used representative values for similar systems taken from the literature, $1x10^{-4}$ for both hydrogen and helium,[14] and $1x10^{-3}$ for oxygen.[15,16]

The effect of zero point energy (ZPE) on the relative hydrogen site stability was considered by estimating the ZPE contribution, within the harmonic approximation, for the octahedral and tetrahedral configurations. For the ZPE calculations, the erbium atoms were assumed stationary and the dynamical matrix was calculated with 24 degrees of freedom (eight hydrogen atoms) in the ideal case and 27 degrees of freedom (nine hydrogen atoms) for octahedral occupation. The dynamical matrix was then diagonalized and the resulting frequencies were used to compute the ZPE.

III. HYDROGEN SITE OCCUPATION AND MIGRATION

The β-phase of erbium hydride has an ideal gas/metal ratio of 2.0, where hydrogen occupies all of the tetrahedral interstitial sites while the octahedral interstices remain unoccupied. Figure 1 shows a conventional unit cell (CaF_2 structure) of β-ErH_2 with tetrahedral hydrogen (blue atoms) and face-centered cubic (fcc) erbium atoms (grey atoms). An empty octahedral site is located at the center of this cell. In each unit cell, there are four fcc lattice sites (1/2 in the center of each cube face and 1/8 in each corner), eight tetrahedral sites, and four octahedral sites (1 in the center and 1/4 on each cube edge). The stoichiometry of any real material will deviate from the perfect 2.0, and, furthermore, even with an ideal stoichiometry, thermal and entropic considerations will lead to finite numbers of tetrahedral vacancies (V_{Tet}) and octahedral interstitials (H_{Oct}).

The DFT calculations of static atomic configurations do not differentiate between hydrogen, deuterium, and tritium isotopes. We considered dynamical effects stemming

from the different atomic masses of these three species by estimating zero point contributions, as described in Section II. The contribution of ZPE to the relative stability of two atomic configurations can be examined by calculating the difference in ZPE per particle for each of the two configurations ($\Delta ZPE = ZPE_{Oct} - ZPE_{Tet}$). Within the harmonic approximation, the vibrational frequency (and magnitude of the ZPE contribution) is expected to scale inversely with the square root of the isotope mass ($\sim 1/(mass)^{1/2}$), and in this case, ΔZPE for H, D, and T are computed to be 7.6, 5.3, and 4.5 meV respectively. Even for H, the lightest isotope, the contribution has an insignificant effect at any reasonable temperature on the relative stability of these two sites.

The relative insignificance of the ZPE contribution to hydrogen site stability in ErH_2 is in contrast with the case of a single hydrogen atom in a metal lattice, where one only need consider the local modes of a single hydrogen atom. In such a system, the ZPE contribution to site stability and migration barriers can be more than 100 meV,[17,18] because the vibrational modes of H_{Oct} are much softer than for H_{Tet}. However, the circumstances are different in erbium dihydride where hydrogen modes are coupled to those of nearby hydrogen, and while the computed local modes for H_{Oct} are indeed softer, those for the surrounding eight H_{Tet} become stiffer than the bulk—compensating in the frequency sum and resulting in only a small difference in ZPE between the two sites. Unless noted, the total energies in this report are given without ZPE contributions.

Using density functional methods, we have calculated the total energy and corresponding equilibrium atomic configuration for the β-phase of ErH_2. We have also investigated several meta-stable configurations including that of one hydrogen occupying an octahedral site (H_{Oct}) leaving a vacant tetrahedral site (V_{Tet}). The pair must be separated by at least one nearest neighbor position, since we find that hydrogen is not locally stable in the octahedral site if there is a neighboring tetrahedral vacancy. If hydrogen is taken from a tetrahedral site and placed in a nearest neighboring octahedral site, it will relax without an energy barrier back to the tetrahedral site. However, hydrogen may become trapped in the octahedral site—a meta-stable condition—if all neighboring tetrahedral sites are filled. This meta-stable configuration (1.21 eV above the ground state) is essentially a Frenkel pair.

Hydrogen site occupation has technological implications regarding phase stability and impurity migration, which are the central subjects of this report. The ratio H/Er also determines the electronic properties, but that topic is beyond the scope of our study.[19] In a tetrahedral site, hydrogen has four nearest neighbors that are all Er metal atoms. While in an octahedral site (octahedrally coordinated with respect to the Er lattice), there are eight nearest neighbors and they are all hydrogen (see Figure 1). When one considers the nearest neighbor interactions of each site, it is not surprising that the octahedral site is less stable or that the material properties are affected by changes in hydrogen site occupation.

A schematic of a low temperature portion of the hydrogen-erbium phase diagram, where the β-phase boundaries are taken from Lundin,[20] is shown in Figure 1. When the gas/metal ratio is less than 2.0, hydrogen will seek its ground state in the tetrahedral sites. Tetrahedral vacancies will exist, and if H/Er drops below 1.85, precipitation of the hexagonal α-phase is thermodynamically favored and may occur provided that migration of V_{Tet} is not kinetically hindered. When the gas/metal ratio exceeds 2.0, additional hydrogen will occupy the octahedral positions. At a gas/metal ratio of about 2.15, excess hydrogen drives a change to the γ-phase. Because the α- and γ-phases are hexagonal, while the β-phase is cubic, a transition from β to either phase may be catastrophic for the physical integrity of the solid, or depending on the mechanical properties, configurationally induced strain might extend the equilibrium boundaries beyond those shown in the schematic. The pure β-phase is stable over a relatively small region of gas/metal ratio. In other words, only a small fraction of V_{Tet} or H_{Oct} can be tolerated before precipitation of a second phase becomes thermodynamically favored. Our calculated migration barriers directly appertain to precipitation of a second phase, which will be mediated by the ability of V_{Tet} or H_{Oct} to congregate.

The climbing image nudged-elastic band (CINEB) method, [13] within DFT, was used to investigate hydrogen migration mechanisms. From these calculations, it is apparent that different hydrogen diffusion mechanisms dominate for different gas/metal stoichiometries. As a result, under-loaded (H/Er < 2.0) and over-loaded (H/Er > 2.0) erbium hydride will exhibit different temperatures where significant hydrogen self-diffusion can occur. The NEB data from relevant transitions are shown in Figure 2. The

details of the mechanism are illustrated in Figure 3 along with a potential energy sketch derived from the data shown in Figure 2.

In the ideal stoichiometric case, where the gas/metal ratio is 2.0, only tetrahedral sites are filled. However, with sufficient energy, hydrogen might jump into a neighboring octahedral site. Because it is not locally stable in the octahedral site, if it is to remain in this position a second hydrogen atom must hop in concert into the newly vacant tetrahedral (V_{Tet}) site, trapping the first hydrogen in the octahedral site (H_{Oct}). Figure 3(a) illustrates this mechanism of thermally generated V_{Tet} and H_{Oct} pairs and possible subsequent migration of the individual species, (b) for the migration of H_{Oct} and (c) for the migration of V_{Tet}. Hydrogen self-diffusion in an ideal (or near ideal) β-phase material is an activated process limited by the formation of the defect pair rather than the diffusion barriers of the individual species.

The associated energy barrier predicted by DFT is 1.90 eV and the formation energy of the defect pair (1.21 eV) is illustrated as (d) in the potential energy diagram of Figure 3. We therefore predict that prohibitively high temperatures are required for significant concentrations of V_{Tet} and H_{Oct} to be thermally generated. Beyond the kinetic limitation, the predicted equilibrium concentration of these defects is small. Using a simple estimate for the equilibrium concentration of Frenkel pairs, $n = (NN')^{1/2}\exp(-1.2/2kT)$, where n is the concentration of pairs, N is the concentration of tetrahedral sites, N' is the concentration of octahedral sites, 1.2 is the formation energy of the pair (occupation energy), k is the Boltzmann constant, and T is the temperature, the estimated equilibrium

concentration is 10^{18} per cm^3 at 500°C. Once a pair is formed, the more mobile H_{Oct} is free to move about, but the barrier to recombination with a vacant tetrahedral site is 0.69 eV and it will likely become recaptured. Thus, movement of hydrogen throughout an ErH_2 film will more likely result from non-stoichiometry such as under-loading, over-loading, or impurity induced H_{Oct}.

From the lower phase boundary of β-ErH_2 until an H/Er ratio of 2.0 is reached, hydrogen will diffuse by movement of V_{Tet}. The mechanism for V_{Tet} migration is illustrated in Figure 3(a) and has a rate limiting barrier of 0.98 eV. An interesting implication of this prediction is that no diffusion of V_{Tet} will occur near room temperature, estimated by the techniques discussed in Section II. In order for significant V_{Tet} diffusion to occur, of up to a micron, sustained temperatures greater than 300 °C are necessary. This is an especially interesting finding in the case of tritium loaded erbium films, where a constant supply of V_{Tet} is created as tritium decays to helium. Because diffusion of V_{Tet} does not occur near room temperature, we predict that precipitation of the α-phase is hindered during normal aging, and an impurity rich β-phase remains meta-stable well below the gas/metal ratio that would otherwise result in phase transition. These inferences will be modified in the presence of helium, as discussed in Section IV. The presence of helium certainly complicates the analysis of V_{Tet} behavior, but should, if anything, serve to further hinder migration of V_{Tet} and precipitation of the α-phase.

Above H/Er = 2.0 and until the β-γ phase boundary, there is an increasing concentration of H_{Oct}. These H_{Oct} can diffuse by jumping into a neighboring (occupied) tetrahedral site,

displacing that hydrogen into the next octahedral site. This *concerted-motion* mechanism is illustrated in Figure 3(b). The barrier for this mechanism was determined to be 0.62 eV, sufficiently small to allow considerable diffusion at relevant temperatures. One hour at 25ºC (100ºC), gives an estimated diffusion length of 0.084 µm (0.95 µm).

In the previous section, we asserted that the contributions of ZPE to the total energy would not effect the interpretation of our results. However, in mixed isotope materials, the differences in ZPE could promote isotopic site separations at low temperatures. Such a site separation, H_{Oct} and D_{Tet}, has indeed been observed in rare earth dihydrides by neutron diffraction and neutron vibrational spectroscopy.[21] In the cited reference, the author noted that the degree of isotopic site separation increased with decreasing temperature and that below ~150K the configuration could be frozen. Even though these experiments were not performed on erbium, it is noteworthy that 150K is near the temperature where our calculated H_{Oct} self-diffusion barrier would predict a lower-bound cutoff for migration.

In summary, hydrogen preferentially resides in the tetrahedral sites before occupying octahedral interstices. The existence and specific concentration of V_{Tet} and H_{Oct} will govern the migration behavior of hydrogen. In under-loaded material, hydrogen diffusion will be dominated by the V_{Tet} mechanism, while in overloaded material, diffusion will be dominated by the *concerted-motion* H_{Oct} mechanism.

IV. HELIUM

In the case of ErT_2, a complicating factor is the short (12.3 years) half-life of tritium, which results in the substantial buildup of impurity helium. The problem being that helium is inert, and will certainly be detrimental to the physical integrity of the host tritide. In addition, the release of helium from the solid into the vacuum of the device can be catastrophic to component functionality. It would be ideal if this mode of aging related material degradation could be precisely predicted, and as such it is important to understand the fundamental atomistic behavior of helium in metal tritides (and hydrides).

In material containing helium from tritium decay, there is initially a V_{Tet} associated with every helium atom produced. The newly created helium atom could occupy the tetrahedral site vacated by a decayed tritium, or it could prefer one of the neighboring octahedral sites. Our calculations predict that helium will occupy the tetrahedral site (He_{Tet}) rather than the octahedral site (He_{Oct}) and is not locally stable in an octahedral site neighboring an empty tetrahedral site. The helium atom is bound to the tetrahedral vacancy by 0.49 eV, with a prohibitive 1.31 eV dissociation energy. The NEB results for helium in erbium hydride are shown in Figure 4 and illustrated in Figure 5 and Figure 6. The energy barrier for motion between two tetrahedral sites (unoccupied by hydrogen) is only 0.49 eV (indicated as (c) in the figures), and as such, even at room temperature helium should move freely between vacant tetrahedral sites. In material where tritium decay continuously produces tetrahedral vacancies, neighboring vacancies are not unlikely, and even an extended network of neighboring vacancies could exist. Such a network would great enhance the range of helium migration.

The NEB data for paths (a) and (b) in Figure 4 resulted from the SeqQuest code, while the data for path (c) results from VASP. The energies of the initial, final, and transition configurations were confirmed in each case with the alternate code (better than 0.025 eV agreement). In Figures 5 and 6, tetrahedral sites not occupied by hydrogen are labeled as T, while those occupied by hydrogen are labeled T*.

The alignment in of potential energy, including the shoulder shown in Figure 6, between helium trapped in a vacancy and dissociation to a region of stoichiometric ErH_2 was confirmed by an NEB calculation between the site T and a neighboring site T* in the figure. The shoulder in this barrier for dissociation, which is spatially near an octahedral site has an energy of 0.40 eV.

If helium impurities exist that are not associated with the decay of a tritium atom, or if helium migrates to a region where the material is stoichiometrically ideal, the energetics of helium site occupation are very different. In this case, the tetrahedral sites are occupied, requiring helium to either reside in an empty octahedral site or displace hydrogen. The energetic price of displacing hydrogen is 0.75 eV (0.73 calculated with VASP), making it much more favorable for helium to occupy the octahedral sites. Energetics, obtained with the NEB method, of the migration path and barrier for displacement of tetrahedral hydrogen by helium are shown in Figure 4(b). After making such a transition, diffusion of helium can proceed by transition to a tetrahedral site different from the initial configuration and continuing to make transitions between empty

octahedral and filled tetrahedral sites. As can be seen in Figures 4 and 5, migration by this mechanism has a lower rate-limiting barrier ((b) 0.88 eV) than the conceptually straight forward mechanism of direct octahedral to octahedral transitions ((a) 1.50 eV), and will be the more dominant mechanism for helium diffusion through ErH_2 where V_{Tet} are not present. We note that this barrier is also relevant to the previous discussion of helium being trapped in a tetrahedral vacancy, since once helium dissociates from the vacancy (or network of vacancies) it must diffuse through material where the tetrahedral sites are occupied.

As was done for hydrogen, the Arrhenius equation was used to estimate diffusion lengths for helium in ErH_2. Diffusion of helium in the hydride or tritide will depend on stoichiometry and/or the amount of tritium decay because the number and distribution of tetrahedral vacancies will determine the rate limiting mechanism. In the case where helium is diffusing through a material with few or no V_{Tet}, the dominant mechanism will involve transitions between empty octahedral sites and filled tetrahedral sites, a process requiring a temporary displacement of H_{Tet}. This process has a rate-limiting barrier of 0.88 eV. Using this barrier, an estimate of the diffusion length for a time of 60 minutes at 300°C is 2.04 μm. Another interesting estimate for analysis of aging tritide films would be 25°C and 10 years, which gives a helium diffusion length of 0.17 μm. These estimates are only valid for a uniform material and actual diffusion lengths may vary drastically from this prediction due to the presence of traps (V_{Tet}), impurities, or variations in stoichiometry. In the tritide, the number of V_{Tet} will be continuously increasing over time as the tritium decays into helium, vacating the tetrahedral sites. After a long time, it is

possible that large extended networks of near neighbor V_{Tet} will allow for wholesale room temperature migration of helium throughout the film. This simple exercise also neglects the presence of other helium traps, the interactions of multiple helium atoms, and the formation of helium bubbles. A future computational analysis will take all of these factors into consideration simultaneously. Nevertheless, our present calculations will serve as a basis for interpretation of future results and serve as a first look into the atomistic processes governing aging of tritium loaded erbium.

V. OXYGEN IMPURITIES

Impurity oxygen has been observed in $Er(D,T)_{2+x}$ films with electron microscopy, energy dispersive spectroscopy, and x-ray diffraction.[1] When this material is annealed (≥250°C), oxide particles form. It is not yet clear if oxygen migrates from the substrate, is inadvertently introduced during erbium deposition and subsequent hydriding, or if it simply migrates from the surface at some point. Moreover, the impacts on material performance and component functionality are probably not fully appreciated. In any case, there is merit in understanding the atomistic behavior of oxygen in erbium hydride, and our calculations and resulting insights move toward that goal.

Using first principles density functional methods, we have determined the most stable local atomic arrangement of oxygen in ErH_2. Instead of occupying empty octahedral sites (O_{Oct}), oxygen prefers the tetrahedral site (O_{Tet}), even though it must displace hydrogen in order to have it. The atomic configuration of O_{Tet} and the associated

displaced hydrogen (H_{Oct}) is shown in Figure 7 along with details of three possible migration mechanisms. The energetics of oxygen moving between a tetrahedral and octahedral site are shown in Figure 8 path (c). The difference in energy between the two sites is 0.50 eV, with a 1.19 eV barrier between them.

Even when a tetrahedral site is already occupied by hydrogen, oxygen will force the hydrogen into a neighboring octahedral site. Thus, each impurity oxygen potentially creates an octahedral hydrogen occupancy. If oxygen were to cluster, forming an oxide particle, the nearby hydride would be locally overloaded with a H/Er > 2.0. Furthermore, if the bulk concentration of oxygen is several percent, the overall number of filled octahedral sites will be increased by that amount. This might have implications for phase stability, if the material is already near the upper boundary where γ-phase precipitation becomes thermodynamically favored. Also, referring back to the data in Figure 2, the rate limiting barrier for migration of octahedral hydrogen is much lower than for tetrahedral hydrogen. Increasing the octahedral occupancy has the additional effect of enhancing the self-diffusion of hydrogen.

From the experimental observation of oxide particle formation, we know that oxygen diffuses at moderate temperatures. Our calculations have identified the likely mechanism--transitions between O_{Tet} and the meta-stable O_{Oct} (E_a = 1.19 eV), path (c) in Figures 7 and 8. During these transitions, hydrogen is forced out of the way, going into and out of H_{Oct} as the oxygen passes by. A direct tetrahedral to tetrahedral transition is less likely (1.58 eV barrier, path (b)), but energetically possible at elevated temperature. Direct

octahedral to octahedral transitions (a) have a prohibitive barrier of 2.90 eV in addition to the barrier associated with first hopping into the octahedral site. At or near room temperature, oxygen will remain immobile but at temperatures above 250°C, oxygen diffusion becomes more significant. We estimate a 0.27 μm diffusion length at 300°C for 60 minutes, which is in excellent agreement with the empirical onset of oxide particle formation during annealing.[1]

VI . SUMMARY AND CONCLUSIONS

The ground state for hydrogen in β-ErH_2 is the tetrahedral site. Displacing hydrogen from the tetrahedral to the neighboring octahedral site costs 1.21 eV in energy, but hydrogen may be trapped in this meta-stable state if no neighboring tetrahedral sites are vacant. In over-loaded films (H/Er > 2.0), hydrogen will occupy octahedral sites since there are no tetrahedral sites available. In under-loaded or stoichiometric films, H_{Oct} may exist due to thermally generated H_{Oct}-V_{Tet} pairs or due to impurities such as oxygen.

Substantial hydrogen migration will depend on non-ideal stoichiometry and/or the presence of impurities that create octahedral hydrogen occupation. While H_{Oct} migration can occur near room temperature, the V_{Tet} mechanism will require temperatures above 200°C. If the stoichiometry is near ideal, hydrogen diffusion will be limited by defect pair formation, which will not be significant until temperatures well over 500°C. This means that in materials where the H/Er ratio is very near 2.0, hydrogen migration will be minimal unless high temperature annealing occurs or impurities are present.

Oxygen impurities prefer the tetrahedral sites and will eject hydrogen into a meta-stable H_{Oct} location. This increases the number of H_{Oct} and will enhance hydrogen diffusion throughout the material. Oxygen will primarily diffuse via hops between octahedral and tetrahedral sites forcing hydrogen, in *concerted-motion*, out of the way as it proceeds. This process can occur at fairly moderate annealing temperatures (~250°C). Direct tetrahedral to tetrahedral hops are not energetically favored, but this mechanism may become active at higher temperatures.

Helium created by tritium decay will seek its ground-state in a vacant tetrahedral site where it will likely be trapped, bound by 0.49 eV. If a connected network of vacant tetrahedral sites exists, helium migration throughout the network will occur at room temperature. Dissociation from this trap has a barrier of 1.31 eV, and the rate limiting barrier for migration beyond this volume is predicted to be 0.88 eV. In order to migrate through the stoichiometric β-phase, helium must move into an empty octahedral site and diffuse by octahedral-tetrahedral-octahedral jumps, forcing H_{Tet} temporarily out of the way as it proceeds. At this point, our calculations do not provide a clear mechanism for helium bubble formation, but future calculations are designed to provide insight.

ACKNOWLEDGEMENTS

Sandia is a multiprogram laboratory operated by Sandia Corporation, a Lockheed Martin Company, for the United States Department of Energy's National Nuclear Security Administration under Contract DE-AC04-94AL85000.

REFERENCES

[1] C.S Snow, L.N Brewer, D.S. Gelles, M.A. Rodriguez, P.G. Kotula, J.C. Banks, M.A. Mangan, and J.F. Browning, J. Nucl. Mater. doi:10.1016/j.jnucmat.2007.07.021 (2007).

[2] J.P. Perdew, K. Burke, and M. Ernzerhhof, Phys. Rev. Lett. 77, 3865 (1996).

[3] P.A. Schultz, unpublished; For additional information, see http:/dft.sandia.gov/Quest/

[4] N. Troullier, J.L Martins, Phys. Rev. B 43, 1993 (1991)

[5] D.R. Hamann, Phys. Rev. B 40, 2980 (1989).

[6] M. Fuchs and M. Scheffler, Comput. Phys. Commun. 119, 67 (1999)

[7] D.R. Hamann, unpublished

[8] G. Kresse and J. Hafner, Phys. Rev. B 47, 558 (1993); G. Kresse and J. Hafner, Phys. Rev. B 49, 14521 (1994); G. Kresse and J. Furthmuller, Comput. Mater. Scie. 6, 159 (1996).

[9] G. Kresse, and J. Jouber, Phys. Rev. B 59, 1758 (1999).

[10] S.G. Louie, S. Froyen, and M.L. Cohen, PRB 26, 1738 (1982)

[11] H.J. Monkhorst and J.D. Pack, Phys. Rev. B 13, 5188 (1976).

[12] J.A. Grimshaw, F.J. Spooner, C.G. Wilson, and A.D. McQuillan, J. Mater. Sci. 16, 2855 (1981).

[13] G. Henkelman, B. Uberuaga and H. Jonsson, J. Chem.Phys. 113, 9901 (2000).

[14] G. Major, J. Gottwald, D.T. Peterson, and R.G. Barnes, J. Alloy. Comp. 330-332, 348 (2002).

[15] R. Stumpf, C.-L. Liu, and C. Tracy, Phys. Rev. B 59, 1 6047 (1999).

[16] J Gegner, G. Horz, and R. Kirchheim, Interface Science 5, 231 (1997).

[17] X. Ke and G.J. Kramer, Phys. Rev. B 66, 184304 (2002).

[18] P. Kamakoti and D.S. Scholl, Journal of Membrane Science 225, 145 (2003).

[19] P. Vajda, Hydrogen in rare earth metals including RH2+x phases, in: K.A. Gschneidner (Ed.), Handbook on the Physics and Chemistry of Rare earths, North-Holland Amsterdam, Vol. 20, pp 207-292 (1995).

[20] C. E. Lundin, Trans. Metall. Soc. AIME, 242, 1161 (1968). C.E. Lundin, Trans. Metall. Soc. AIME, 242, 903 (1968).

[21] T.J. Udovic, Q. Huang, and J.J. Rush, Phys. Rev. B 62, 6611 (2000)

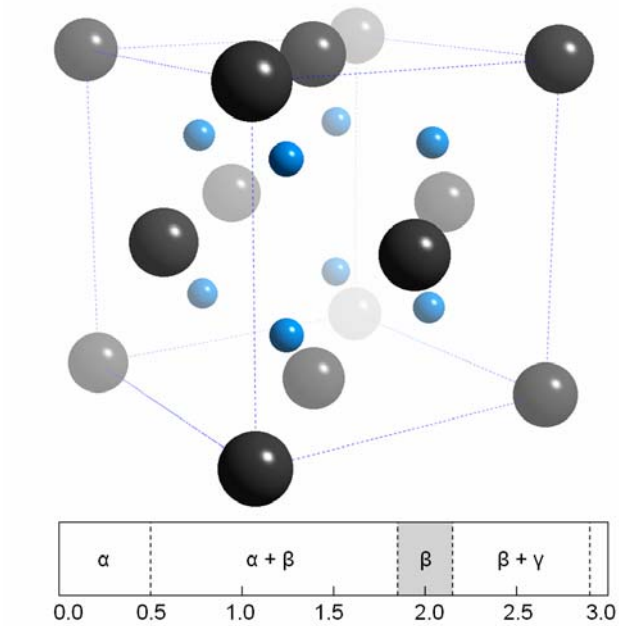

FIG 1. (color online) A unit cell of β-ErH_2 and a schematic of the low temperature phase-diagram. The eight smaller blue atoms represent hydrogen occupying all of the tetrahedral sites. The larger grey atoms represent the erbium face-centered cubic lattice. The octahedral sites, in the middle of each cube edge and in the cube center, are unoccupied. The schematic phase diagram is shown in terms of H/Er ratio.

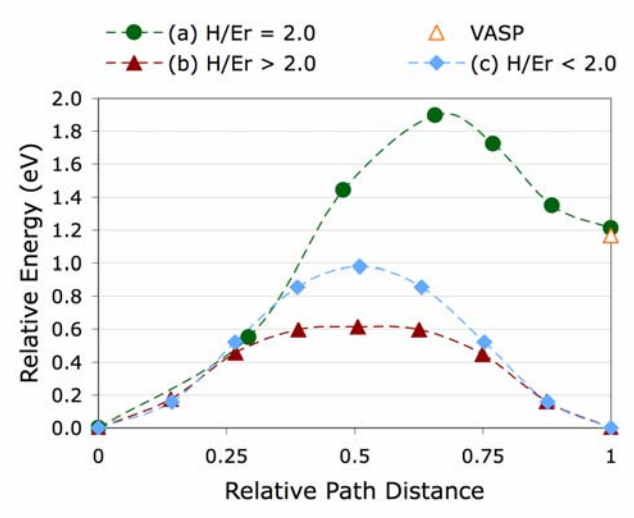

FIG 2. (color online) Climbing-image nudged elastic band (NEB) data for migration of hydrogen in β-ErH_2. Three possible mechanisms are shown. The initial configurations, final configurations, and path motion are illustrated in Figure 3. The dominant mechanism will be determined by the H/Er ratio, which indicates the presence of H_{Oct} and/or V_{Tet}. (a) The barrier and formation energy for the thermal generation of H_{Oct} / V_{Tet} pairs. (b) The barrier for H_{Oct} migration. (c) The barrier for V_{Tet} migration. The open triangle is the final state configuration of path (a) computed with VASP rather than SeqQuest.

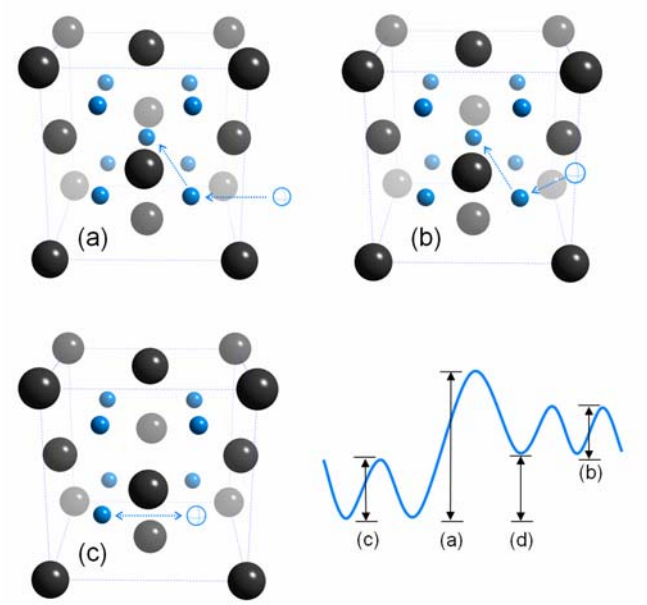

FIG 3. (color online) Illustration of the data in Figure 2 including a potential energy diagram for the mechanisms. (a) Formation of H_{Oct} / V_{Tet} pairs, 1.90 eV. (b) Migration of $H_{Oct,}$ 0.62 eV. (c) Migration of $V_{Tet,}$ 0.98 eV. (d) shows the formation energy 1.21 eV of the Frenkel pair. The hollow blue atoms represent initial positions of hydrogen. The blue atoms are hydrogen and the larger grey atoms are erbium. The blue dotted arrows indicate motion of the atoms along the path.

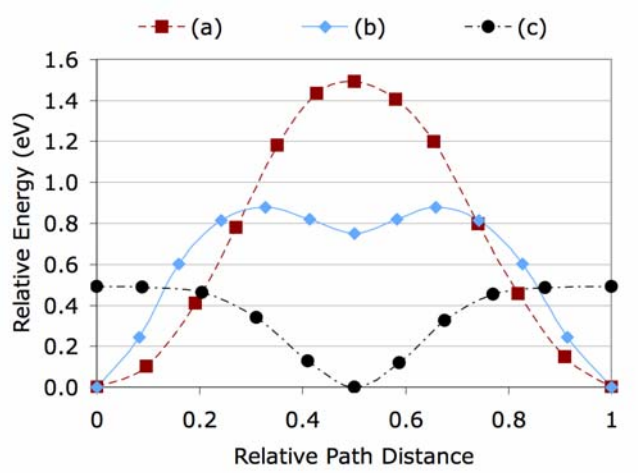

FIG 4. (color online) Climbing image nudged elastic band data for helium migration in ErH_2. (a) Direct octahedral to octahedral migration. (b) Concerted-motion from empty octahedral to a filled tetrahedral position (path distance of 0.5) and on to another empty octahedral site. The energy of the tetrahedral site, 0.75 eV, was also calculated with VASP as 0.73 eV. (c) Migration between octahedral and vacant tetrahedral sites. All of the data is arranged such that a path distance of 0 or 1 is an octahedral site. For paths (b) and (c) 0.5 is in the tetrahedral site, while for (a) it is the direct mid-point between two octahedral sites. The corresponding mechanisms and schematic potential energy are illustrated in Figure 5 and Figure 6 respectively.

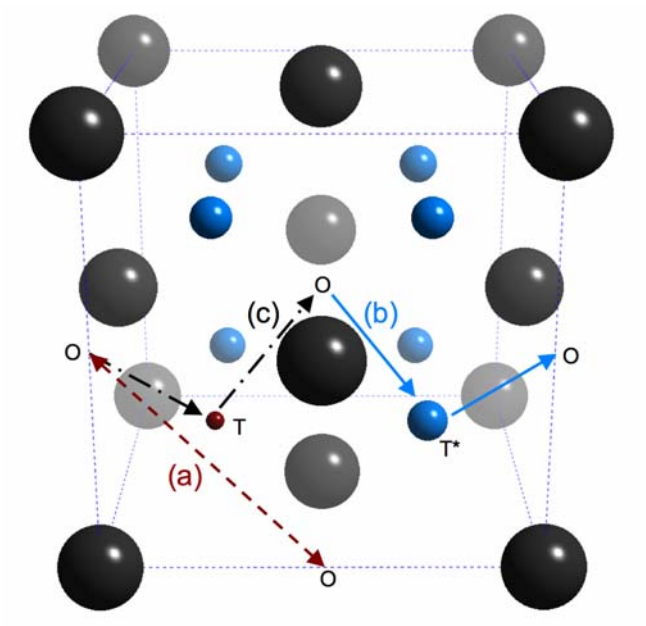

FIG 5. (color online) Illustration of helium migration mechanisms corresponding to the NEB data in Figure 4. (a) The red dashed line indicates direct octahedral (O) to octahedral migration. (b) The blue solid lines shows the motion of helium from octahedral to octahedral through the intermediate filled tetrahedral site T*. (c) The black dash-dot line shows motion of helium from octahedral to octahedral through an intermediate vacant tetrahedral site T (the ground state). The blue atoms are hydrogen, the smaller red atom is helium, and the larger grey atoms are erbium.

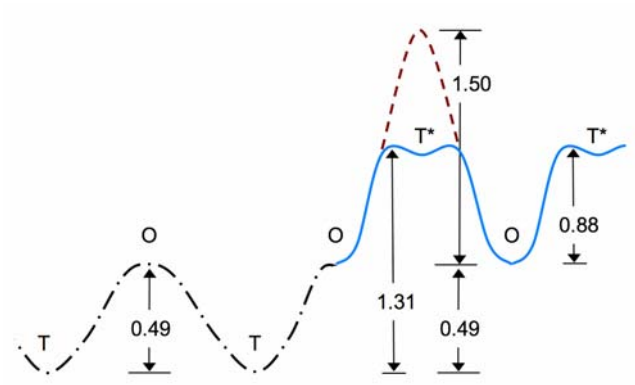

FIG 6. (color online) Schematic illustration and alignment of the helium NEB data from Figure 4. The red dashed line is the barrier for direct octahedral (O) to octahedral migration. The blue solid lines shows the motion of helium from octahedral to octahedral through the intermediate filled tetrahedral site T*, as in stoichiometric β-phase. The black dash-dot line, corresponding to path (c) in Figures 4 and 5, shows the barrier for motion of helium from a tetrahedral site to a neighboring tetrahedral vacancy. The alignment of the left (black dash-dot) and right (blue solid) portions of the diagram was calculated by an additional VASP NEB calculation starting from site T and ending in site T*, providing the barrier of 1.31 eV for dissociation of helium from V_{Tet}. The shoulder in this barrier, at 0.40 eV, does not represent a meta-stable state, but configurationally is near the octahedral position.

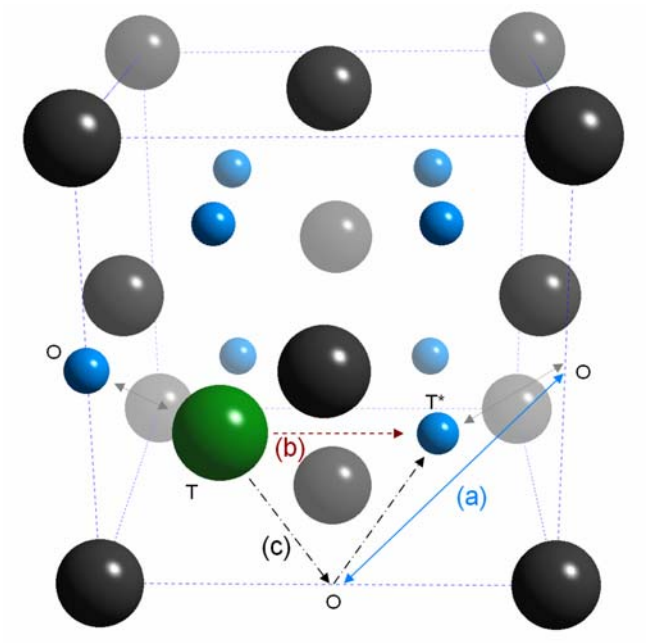

FIG 7. (color online) Migration mechanism for oxygen, the large green atom, located in the tetrahedral site T. (a) Direct octahedral (O) to octahedral motion indicated by the solid blue line. (b) Direct tetrahedral (T) to tetrahedral migration into an already occupied tetrahedral site T*. (c) Movement from the tetrahedral site into an empty octahedral site and on into a filled tetrahedral site T*. Mechanisms b and c involve relaxation of octahedral hydrogen (H_{Oct}) into the initial tetrahedral position, and displacement of the hydrogen in T* into an H_{Oct} configuration (indicated by the grey arrows). NEB data for these mechanisms are shown in Figure 8.

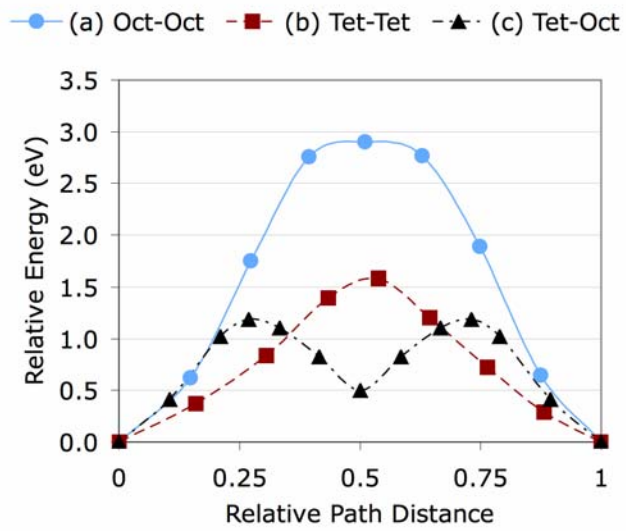

FIG 8. (color online) Nudged elastic band data for migration of oxygen in erbium hydride. (a) Direct octahedral to octahedral migration. (b) Direct tetrahedral to tetrahedral migration. (c) Migration from a tetrahedral site through an empty octahedral site (path distance of 0.5) and on into another tetrahedral site. For paths b and c the initial and final state have an associated H_{Oct} which is illustrated in Figure 7.

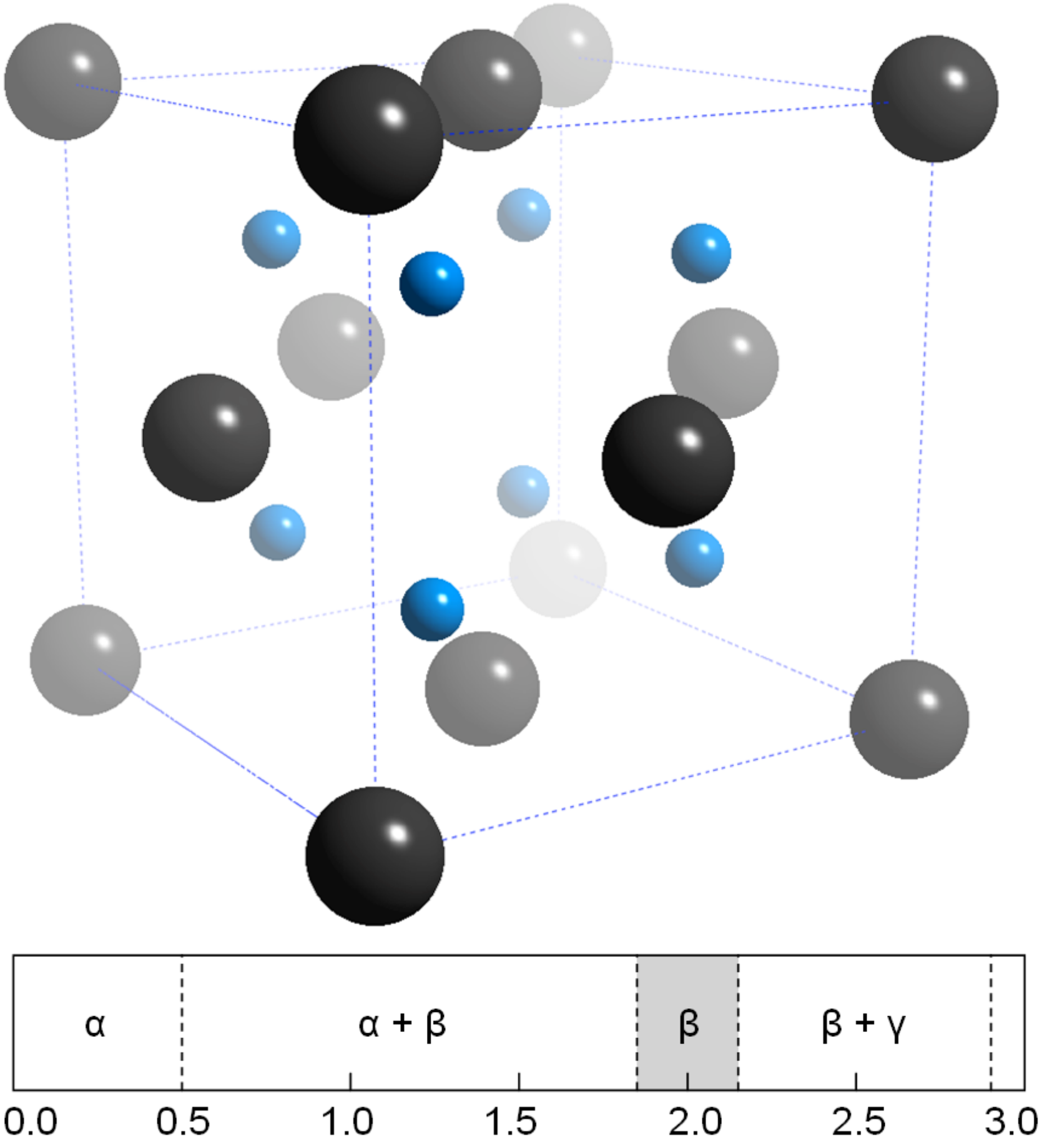
α
α + β
β
β + γ
0.0
0.5
1.0
1.5
2.0
2.5
3.0

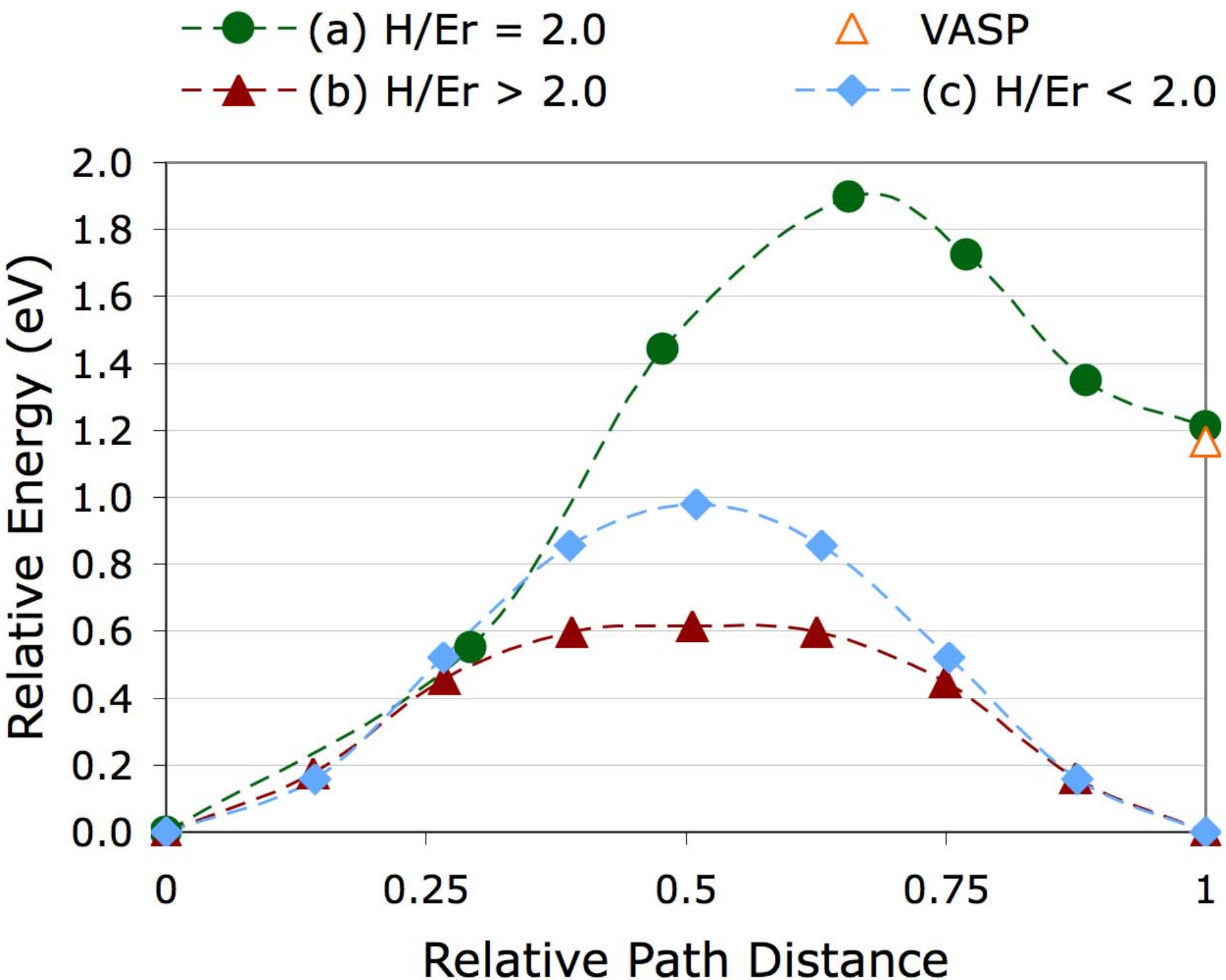
(a) H/Er = 2.0
VASP
(b) H/Er > 2.0
(c) H/Er < 2.0
Relative Energy (eV)
2.0
1.8
1.6
1.4
1.2
1.0
0.8
0.6
0.4
0.2
0.0
0
0.25
0.5
0.75
1
Relative Path Distance

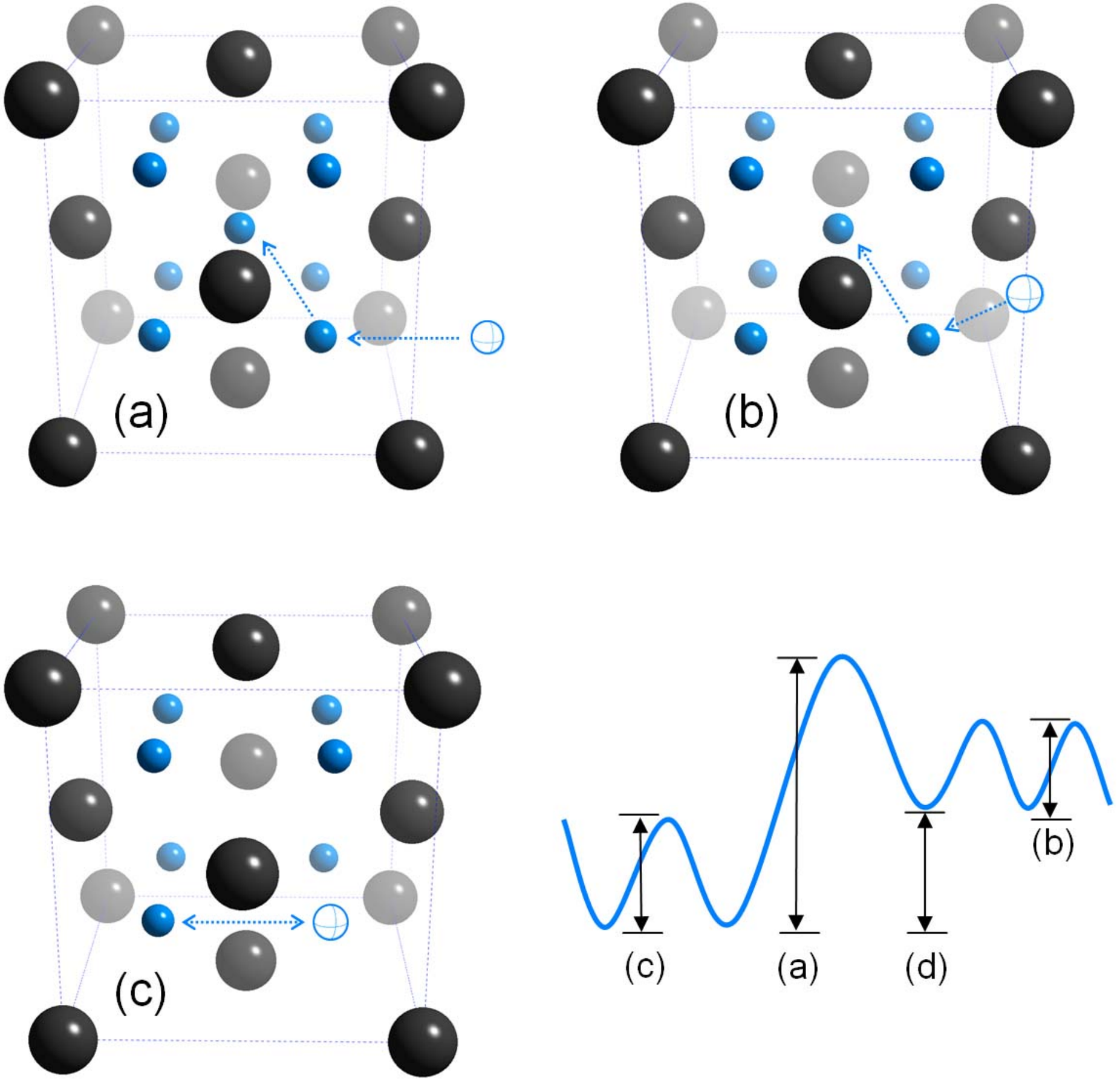
(a)
(b)
(c)
(c)
(a)
(d)
(b)

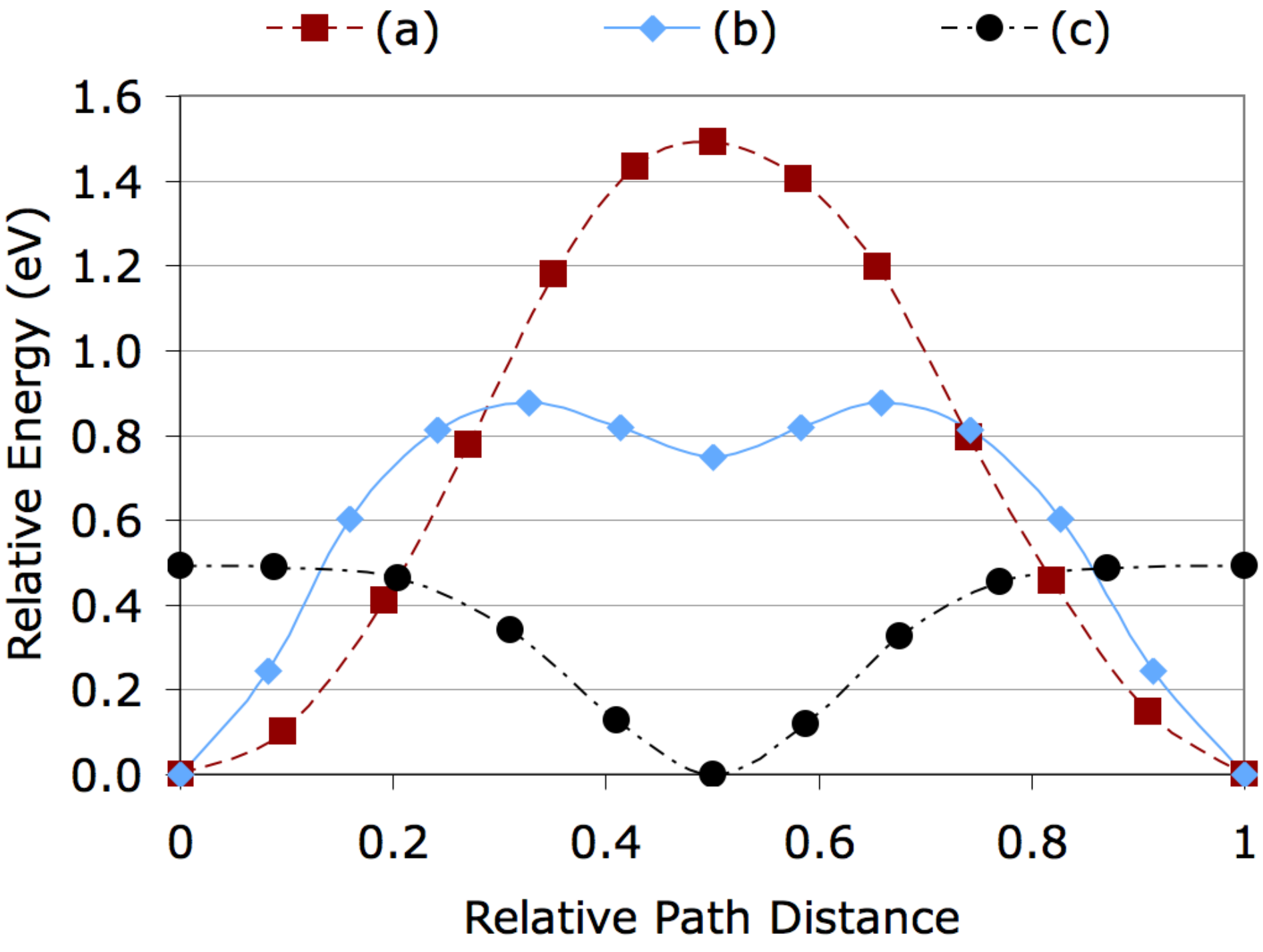
(a)
(b)
(c)
1.6
1.4
1.2
1.0
0.8
0.6
0.4
0.2
0.0
Relative Energy (eV)
0
0.2
0.4
0.6
0.8
1
Relative Path Distance

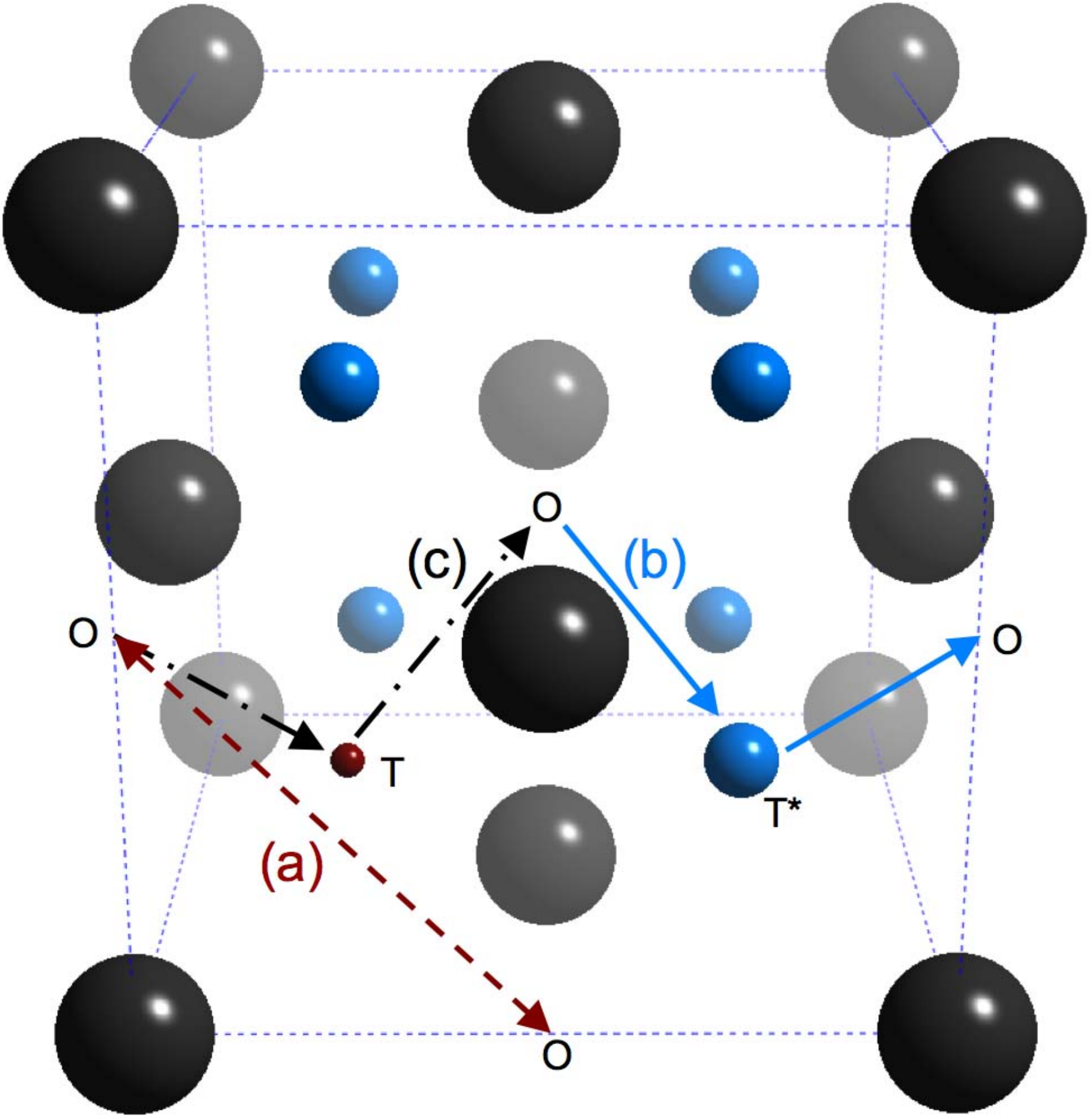
O
(c)
(b)
O
O
T
T*
(a)
O

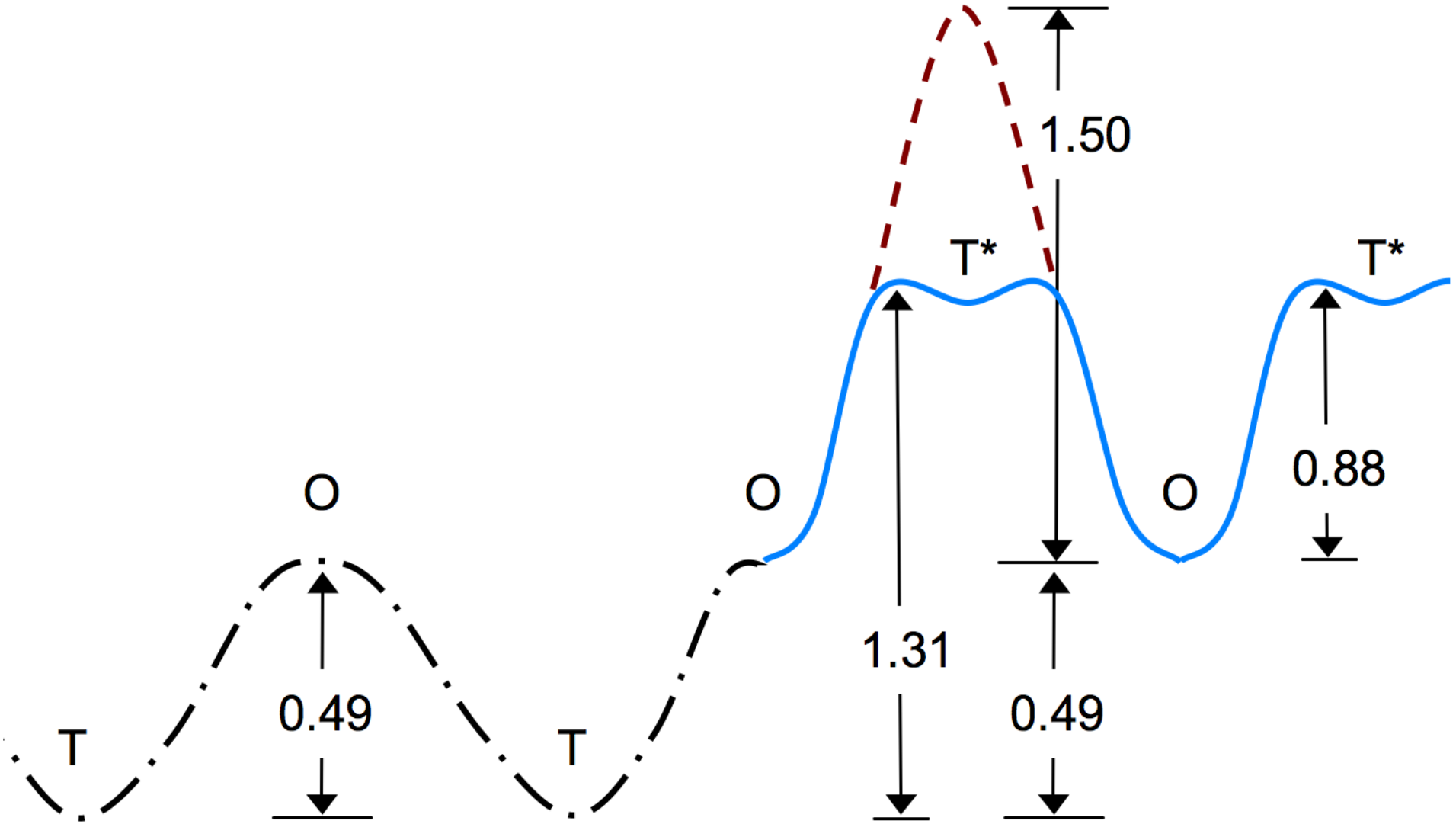
1.50
T*
T*
O
O
O
0.88
1.31
0.49
0.49
T
T

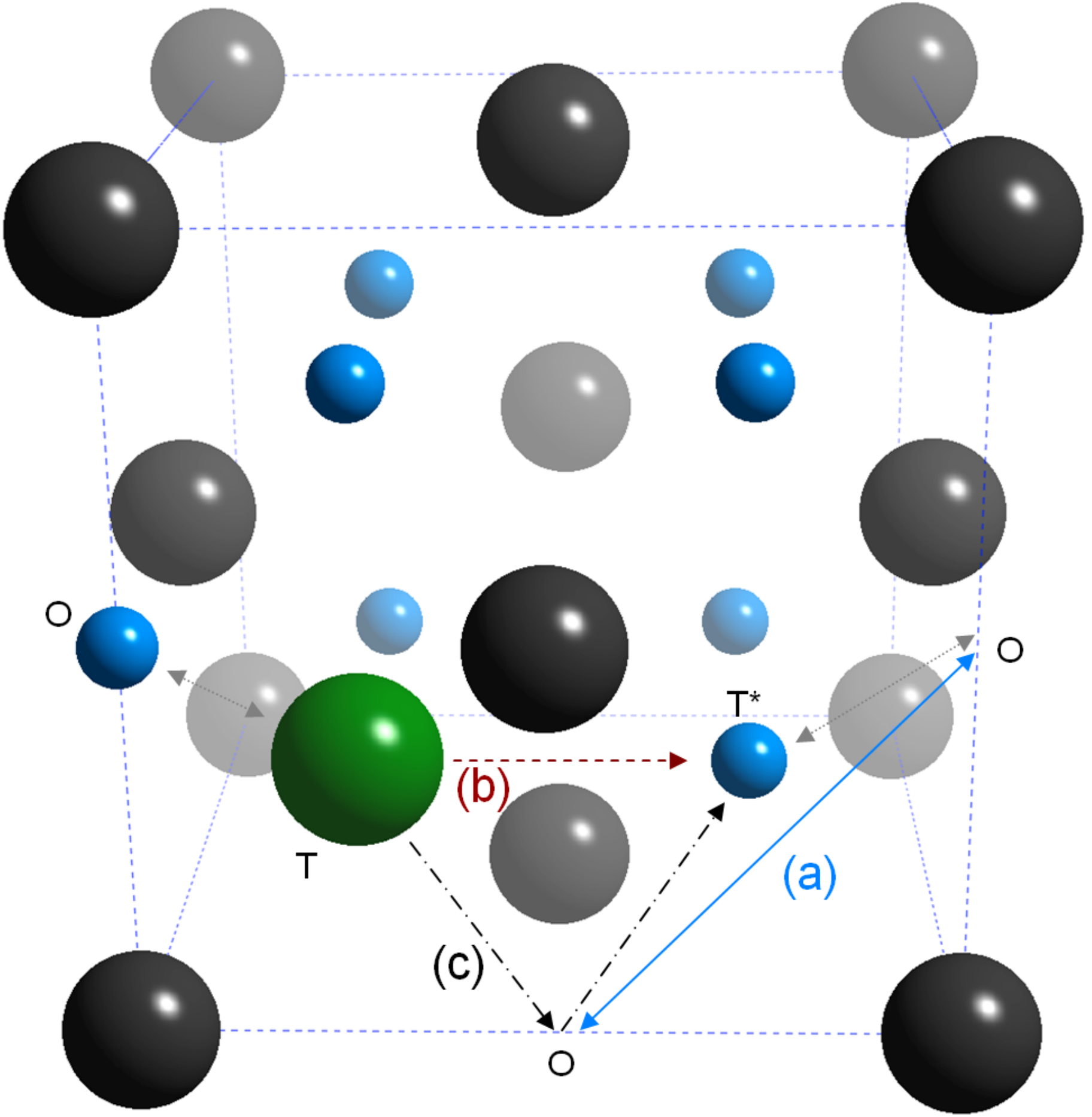
O
O
T*
(b)
T
(a)
(c)
O

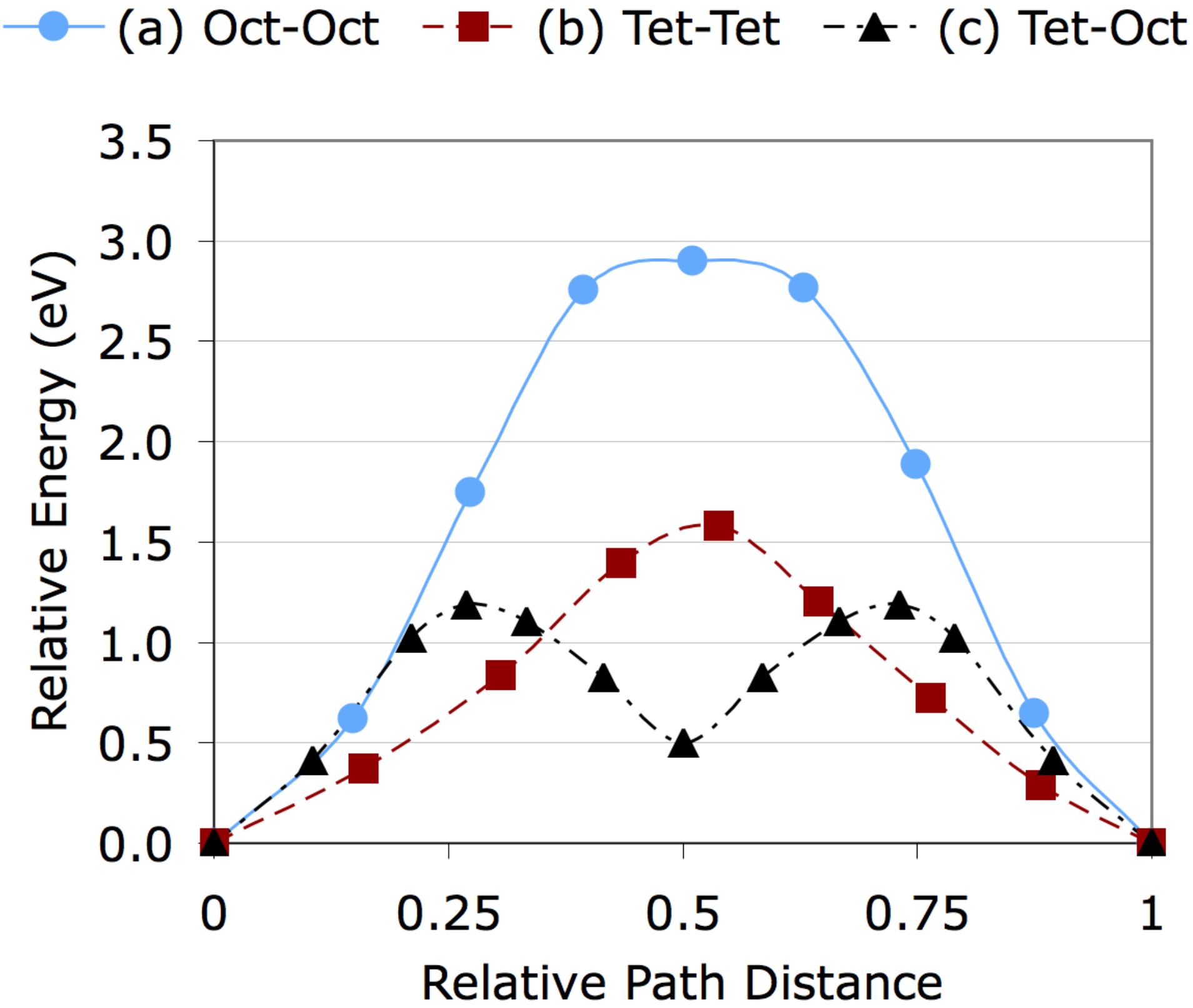
(a) Oct-Oct
(b) Tet-Tet
(c) Tet-Oct
Relative Energy (eV)
3.5
3.0
2.5
2.0
1.5
1.0
0.5
0.0
0
0.25
0.5
0.75
1
Relative Path Distance